

# Kriging as a Means of Improving WAAS Availability

Lawrence Sparks, *Jet Propulsion Laboratory, California Institute of Technology*  
Juan Blanch, *Stanford University*  
Nitin Pandya, *Raytheon Company*

## BIOGRAPHY

**Dr. Lawrence Sparks** is a member of the Ionospheric and Atmospheric Remote Sensing Group in the Tracking Systems and Applications Section at NASA's Jet Propulsion Laboratory. He received his Ph.D. in Applied Physics from Cornell University and has pursued research in various fields including fusion plasma physics, solar magnetohydrodynamics, atmospheric radiative transfer, and ionospheric modeling. He is a member of the WAAS Integrity and Performance Panel and is currently working on issues concerning the impact of the ionosphere on satellite-based augmentation systems.

**Dr. Juan Blanch** received a Ph.D. in Aeronautics and Astronautics in December 2003 from Stanford University, for his work on ionospheric estimation for the Wide Area Augmentation System (WAAS). He has continued as a Research Associate in the Stanford GPS laboratory, where he is currently developing algorithms for civil aviation navigation integrity.

**Dr. Nitin Pandya** is a Senior Systems Engineer at Raytheon Company. He received his B.S. in Physics from the University of California, Los Angeles, and his M.S. and Ph.D. in Physics from the University of California, Irvine. He has been working in GPS and Differential GPS technology since 1997 on the WAAS, MSAS, GAGAN, LAAS, and GPS III systems.

## ABSTRACT

The Wide Area Augmentation System (WAAS), an augmentation of the Global Positioning System (GPS), provides safe and reliable use of GPS signals for airline navigation over much of North America. Currently the largest source of positioning error in the system is signal delay caused by the ionosphere. To allow the user to take account of such error, WAAS computes and broadcasts ionospheric vertical delays at a set of regularly-spaced grid points. In addition, WAAS computes and broadcasts a safety-critical integrity bound at each *ionospheric grid point* (IGP) called the Grid Ionospheric Vertical Error (GIVE). GIVES are constructed to be sufficiently large to

protect the user against positioning error due to the presence of ionospheric irregularity.

In the initial operating capability (IOC) of WAAS, the vertical delay estimate at each IGP is determined from a planar fit of neighboring slant delay measurements, projected to vertical using an obliquity factor specified by the standard thin-shell model of the ionosphere. In WAAS Follow-On (WFO) Release 3, however, the vertical delay will be estimated by an established, geo-statistical technique known as *kriging*. Compared to the planar fit model, the kriging model is found, in general, to match better the observed random structure of the vertical delay. This paper presents the kriging methodology that will be used to estimate the vertical delay and its uncertainty at each IGP, and it assesses the subsequent improvement in WAAS availability enabled by kriging.

## INTRODUCTION

To ensure the safety of airline navigation based upon signals of the Global Positioning System, satellite-based augmentation systems (SBAS) have been developed to guarantee the accuracy, integrity, availability, and continuity of user position estimates derived from GPS measurements. For single-frequency GPS users, ionospheric delay continues to be the largest source of positioning error. In the United States, the Wide Area Augmentation System measures ionospheric slant delays using multiple dual frequency receivers in a network of thirty-eight reference stations distributed across North America (see Fig. 1). To allow the user to correct for the error due to ionospheric delay, WAAS computes from these measurements a set of vertical delays at ionospheric grid points (see Fig. 2) defined by the WAAS Minimum Operational Performance Standards (MOPS) [1]. WAAS also computes a safety-critical integrity bound at each IGP called the Grid Ionospheric Vertical Error. GIVES are derived from inflated values of the formal error and provide protection against delay estimate error that arises from ionospheric irregularity, both sampled and undersampled. WAAS broadcasts the vertical delay estimates and their GIVES at regular intervals in time.

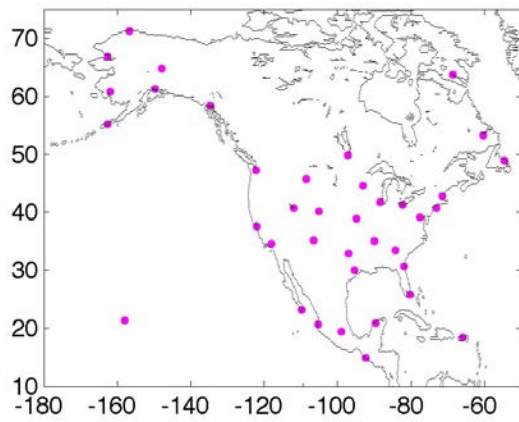


Figure 1. WAAS receiver sites in North America.

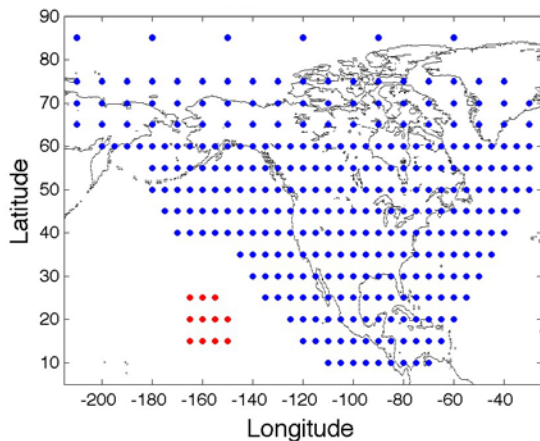


Figure 2. WAAS IGP mask of ionospheric grid points (the blue dots indicate the IGP working set).

Raypaths that connect satellites to receivers determine the sampling of ionospheric irregularities. Associated with each raypath is an *ionospheric pierce point* (IPP) defined as the location where a station-to-satellite raypath penetrates an infinitesimally thin, spherical shell at an altitude of 350 km. The area near an IGP is undersampled when the IPP coverage there is sparse or highly non-uniform. To protect against the effects of undersampling at the IGP, a term is added to the GIVE to bound gradient threats that may be present when the ionosphere is disturbed.

The WAAS undersampled ionospheric threat model [2] consists of a table of values that govern the amount by which the GIVE is inflated to protect against undersampled threats. This table is derived from historical WAAS observations, *i.e.*, from the twenty-one days during the last solar maximum that exhibited the highest levels of ionospheric disturbance. To identify these data sets, it has been assumed that the level of ionospheric disturbance correlates strongly with the level of geomagnetic disturbance as indicated by the geomagnetic indices  $K_p$  and  $D_{ST}$ . To define the threat model, the worst-case undersampled ionospheric gradient threats are tabulated as a function of two metrics that characterize the

IPP distribution (see Fig. 3): the fit radius and the relative centroid metric (*i.e.*, the centroid radius divided by the fit radius).

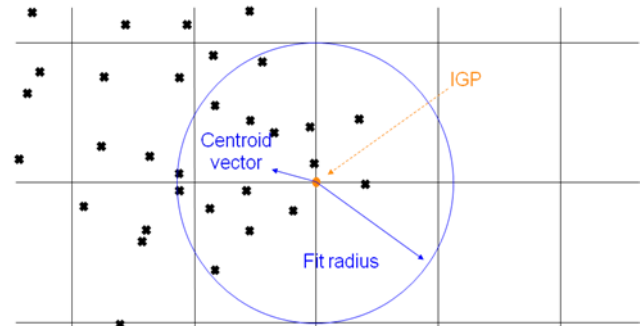


Figure 3. IPP distributions at an IGP are characterized by the *fit radius* and the *relative centroid metric*.

In the initial operating capability of WAAS, a vertical delay estimate is calculated at each IGP from a planar fit of neighboring slant delay measurements, projected to vertical using the standard thin-shell obliquity factor (see Fig. 4). In WAAS Follow-On (WFO) Release 3, the vertical delay estimates will be obtained by a geostatistical technique known as *kriging* [3][4], a type of minimum mean square estimator adapted to spatial data, that originated in the mining industry in the 1950's. Kriging renders a smoothed image of a spatially distributed variable that has been sampled by irregularly spaced measurements. The kriging model generally achieves a better match to the observed random structure of the vertical delays than does the planar fit model (or the kriging model can be tuned to match these data better).

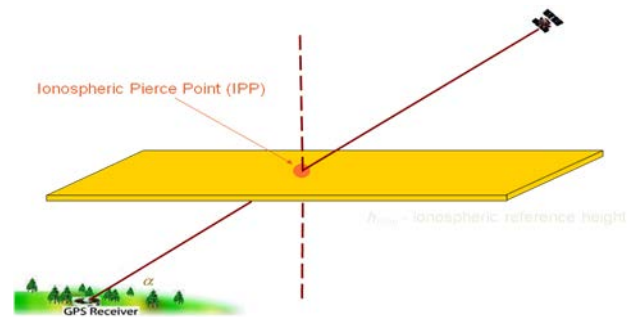


Figure 4. Mapping slant delay to vertical delay assumes the ionosphere occupies a thin shell.

This paper presents the kriging methodology to be used by WAAS for estimating vertical delay and its uncertainty at each IGP. It quantifies the improvement in delay accuracy achieved by kriging and discusses the impact of kriging on the ionospheric threat model. Finally, it concludes by discussing the improvement in availability that is anticipated in the next release of WAAS.

## THE KRIGING EQUATIONS

The kriging estimate of vertical delay at a given location is determined from observations whose IPPs lie in the vicinity of this location. Let us consider a set of  $N_{IPP}$  measurements whose IPPs lie in the vicinity of the  $v^{\text{th}}$  IGP. Let  $\mathbf{I}_{v,IPP}$  designate a vector whose elements represent the corresponding vertical delay values, *i.e.*, slant delay measurements converted to vertical using the standard obliquity factor. Then the kriging estimate  $\tilde{I}_{IGP,v}$  of the ionospheric vertical delay at this IGP is calculated [4] as:

$$\tilde{I}_{IGP,v} = \mathbf{w}_v^T \mathbf{I}_{v,IPP},$$

where the vector of coefficients  $\mathbf{w}_v$  is specified by:

$$\mathbf{w}_v \equiv \left[ \mathbf{W}_v - \mathbf{W}_v \mathbf{G}_v (\mathbf{G}_v^T \mathbf{W}_v \mathbf{G}_v)^{-1} \mathbf{G}_v^T \mathbf{W}_v \right] \mathbf{c}_v + \mathbf{W}_v \mathbf{G}_v (\mathbf{G}_v^T \mathbf{W}_v \mathbf{G}_v)^{-1} [1 \ 0 \ 0]^T.$$

The observation matrix  $\mathbf{G}_v$  is defined as

$$\mathbf{G}_v \equiv \begin{bmatrix} 1 & \Delta \mathbf{x}_{1,v}^T \cdot \hat{\mathbf{E}}_v & \Delta \mathbf{x}_{1,v}^T \cdot \hat{\mathbf{N}}_v \\ 1 & \Delta \mathbf{x}_{2,v}^T \cdot \hat{\mathbf{E}}_v & \Delta \mathbf{x}_{2,v}^T \cdot \hat{\mathbf{N}}_v \\ \vdots & \vdots & \vdots \\ 1 & \Delta \mathbf{x}_{N_{IPP},v}^T \cdot \hat{\mathbf{E}}_v & \Delta \mathbf{x}_{N_{IPP},v}^T \cdot \hat{\mathbf{N}}_v \end{bmatrix}$$

where  $\hat{\mathbf{E}}_v$  and  $\hat{\mathbf{N}}_v$  are the standard East and North unit vectors defined for the Up-East-North (UEN) Cartesian coordinate system with its origin at the  $v^{\text{th}}$  IGP, and

$$\Delta \mathbf{x}_{\kappa,v} \equiv \begin{bmatrix} x_{IPP_\kappa} \\ y_{IPP_\kappa} \\ z_{IPP_\kappa} \end{bmatrix} - \begin{bmatrix} x_{IGP_v} \\ y_{IGP_v} \\ z_{IGP_v} \end{bmatrix}$$

is the Euclidean vector describing the distance separating the  $\kappa^{\text{th}}$  IPP from the  $v^{\text{th}}$  IGP in earth-centered, earth-fixed (ECEF) Cartesian coordinates. A weighting matrix, designated  $\mathbf{W}_v$ , assigns appropriate weights to the individual measurements for the linear estimate; it is defined as

$$\mathbf{W}_v \equiv [\mathbf{M}_v + \mathbf{C}_v]^{-1},$$

where  $\mathbf{M}_v$  is the  $N_{IPP} \times N_{IPP}$  measurement noise covariance matrix and  $\mathbf{C}_v$  is the  $N_{IPP} \times N_{IPP}$  nominal ionospheric covariance matrix at the  $v^{\text{th}}$  IGP. The latter's elements are specified by

$$C_{v,\kappa\kappa} = (\sigma_{decorr}^{total})^2$$

$$C_{v,\kappa l} = \left[ (\sigma_{decorr}^{total})^2 - (\sigma_{decorr}^{nom})^2 \right] \exp(-D_{v,\kappa l} / d_{decorr}), \text{ if } \kappa \neq l,$$

where

$$D_{v,\kappa l} \equiv \sqrt{(\Delta \mathbf{x}_{\kappa,v} - \Delta \mathbf{x}_{l,v})^T (\Delta \mathbf{x}_{\kappa,v} - \Delta \mathbf{x}_{l,v})}$$

and  $\sigma_{decorr}^{total}$ ,  $\sigma_{decorr}^{nom}$ , and  $d_{decorr}$  are parameters that specify the nominal ionospheric decorrelation. The elements in the vector  $\mathbf{c}_v$ , describing the nominal covariance between the IGP and the  $N_{IPP}$  IPPs, are defined as:

$$c_{v,\kappa} = \left[ (\sigma_{decorr}^{total})^2 - (\sigma_{decorr}^{nom})^2 \right] \exp(-d_{v,\kappa} / d_{decorr}),$$

where

$$d_{v,\kappa} = \sqrt{\Delta \mathbf{x}_{\kappa,v}^T \Delta \mathbf{x}_{\kappa,v}}.$$

The formal uncertainty in the vertical delay estimate is given by

$$\sigma_{FE,IGP}^2 = \mathbf{w}^T \cdot \mathbf{C} \cdot \mathbf{w} - 2\mathbf{w}^T \cdot \mathbf{c} + (\sigma_{decorr}^{total})^2 + \mathbf{w}^T \cdot \mathbf{M} \cdot \mathbf{w}.$$

These equations reduce to the planar fit equations used in IOC when  $\sigma_{decorr}^{total}$  is equal to  $\sigma_{decorr}^{nom}$ .

## IMPROVEMENT IN ACCURACY

A standard *goodness-of-fit* statistic characterizes the discrepancy between observed vertical delay values and the values estimated by the model in question. For the planar fit model, the goodness-of-fit statistic can be expressed as

$$\chi_v^2 \equiv \mathbf{I}_{v,IPP}^T \cdot \mathbf{W}_v \cdot (\mathbf{I}_d - \mathbf{P}_v) \cdot \mathbf{I}_{v,IPP}$$

where

$$\mathbf{P}_v \equiv \mathbf{G}_v \cdot (\mathbf{G}_v^T \cdot \mathbf{W}_v \cdot \mathbf{G}_v)^{-1} \cdot \mathbf{G}_v^T \cdot \mathbf{W}_v$$

A similar expression can serve as a basis for characterizing the goodness-of-fit for kriging estimation.

The  $\chi^2$  statistic associated with the estimation of vertical delay at an IGP has been found to be the best indicator of the level of ionospheric irregularity in the vicinity of that IGP. Consequently, it provides a basis for defining an *irregularity metric* that indicates whether it is safe for a user to calculate his or her position using the vertical ionospheric delay estimate associated with this IGP:

$$\chi_{irreg,v}^2 \equiv \frac{R_{noise,v} \chi_v^2}{\chi_{norm}^2},$$

where  $R_{noise,v}$  is an inflation factor that prevents the presence of measurement noise from concealing the magnitude of an ionospheric irregularity, and  $\chi_{norm}^2$  is the inverse  $\chi^2$  cumulative probability distribution function evaluated for a probability of 99.9% and the number of degrees of freedom set to 3. The *irregularity detector* at the IGP is said to have tripped when the irregularity

metric exceeds a threshold value  $T_{irreg,trip}$ . When the irregularity detector at an IGP is tripped, the GIVE at the IGP is increased to 45 meters. A 45 meter GIVE safely bounds the maximum WAAS ionospheric estimation error and represents the maximum GIVE value possible.

A comparison of distributions of the goodness-of-fit statistics for estimation based upon planar fits and kriging shows the improvement in accuracy afforded by kriging. For example, Fig. 5 displays the distribution of  $\chi^2$  for planar fit estimation based upon observational data from November 20, 2003, a date when a major storm occurred and the ionosphere was highly irregular. The maximum value, mean value, and standard deviation for this distribution are 489, 3.3, and 16.6, respectively.

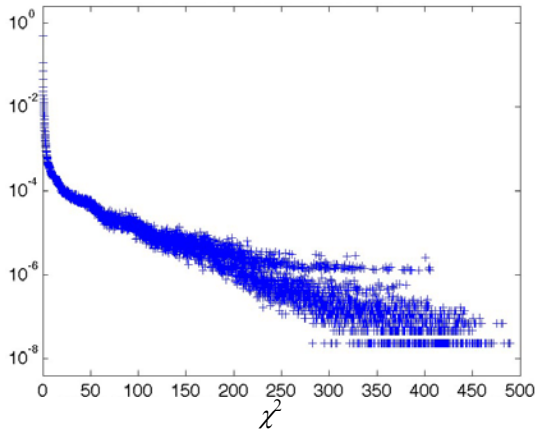


Figure 5. The distribution of  $\chi^2$  for planar fit estimation based upon measurements from November 20, 2003.

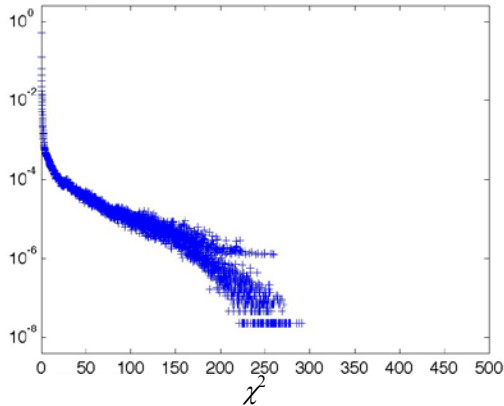


Figure 6. The distribution of  $\chi^2$  for kriging estimation based upon measurements from November 20, 2003.

Figure 6 shows the analogous plot for kriging estimation. In this case, the maximum value, mean value, and standard deviation for this distribution are 291, 2.6, and 12.6, respectively, values considerably smaller than the corresponding values for planar fit estimation. These statistics indicate that estimate accuracy improves dramatically when kriging is implemented.

## INFLATION OF FORMAL ERROR

There is some probability that the statistical uncertainty  $\sigma_{FE,IGP}^2$  underestimates significantly the actual error in the estimated vertical delay at an IGP. To allow for this possibility, the formal error used to evaluate the GIVE is inflated [5]:

$$\sigma_{IGP}^2 = R_{irreg}^2 \left[ \mathbf{w}^T \cdot \mathbf{C} \cdot \mathbf{w} - 2\mathbf{w}^T \cdot \mathbf{c} + (\sigma_{decor}^{total})^2 \right] + \mathbf{w}^T \cdot \mathbf{M} \cdot \mathbf{w}$$

where

$$R_{irreg,v}^2 \equiv \frac{R_{noise,v} \chi_v^2}{\chi_{lowerbound}^2}$$

is an inflation factor used to account for ionospheric and statistical uncertainty in the  $\chi_v^2$  associated with the estimate and  $\chi_{lowerbound}^2$  is a system parameter. Note that this equation reduces to the formal error when  $R_{irreg,v}^2$  is set to unity.

## THE IONOSPHERIC THREAT MODEL

In addition to inflating the GIVEs to account for statistical uncertainty, the GIVEs are also inflated to protect the user from the effects of undersampling ionospheric irregularities. The need for such protection is illustrated by an event that occurred during the *Halloween storm* of 2003. On successive days beginning on October 29, 2003, two coronal mass ejections (CMEs) struck the earth during daylight hours roughly 24 hours apart. These CMEs caused major disturbances in the ionosphere. Normally, the electron density in the ionosphere diminishes to very small values during the night. However, a highly localized remnant of the daytime disturbance persisted for many hours late into the night following the second CME.

Fig. 7 shows the estimated vertical delay over the southeastern United States at 5:00 UTC. The disturbance in question hovers over Florida and hence is referred to as the *Florida event*. Circles indicate the locations of the IPPs associated with the delay measurements used to estimate the vertical delay. The line segment attached to a circle points to the receiver that recorded the measurement. The length of the segment reflects the magnitude of the elevation angle – the longer the segment, the lower the elevation. To illustrate how the irregularity might have gone undetected, the five measurements that actually penetrated the irregularity have been removed. In fact WAAS did detect this irregularity and responded appropriately. No misleading information was broadcast. It is clear, however, that, had the irregularity been located somewhat to the west and slightly south, it might have gone undetected.

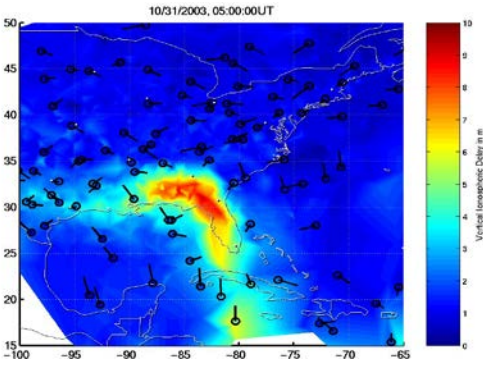


Figure 7. A dense, localized ionospheric irregularity that occurred over Florida at 5:00 UTC on October 31, 2003. Color contours indicate the magnitude of the vertical delay. Circles identify measurement IPPs, and the line segment at each circle points to the receiver that recorded the measurement. The five measurements that sampled the irregularity have been removed. (This figure is provided courtesy of Todd Walter *et al.* [6]).

To protect against the threat posed by undersampling, the GIVE is inflated by introducing a dependence on a term designated  $\sigma_{decorr}^{undersamp}$ . To bound the actual error, the condition to be satisfied can be expressed qualitatively as

$$|I_{IPP_\kappa} - \tilde{I}_{IPP_\kappa}|^2 < K_{undersampled}^2 \sigma_{IPP_\kappa}^2,$$

where  $I_{IPP_\kappa}$  is the measured vertical delay at the  $\kappa^{\text{th}}$  IPP,  $\tilde{I}_{IPP_\kappa}$  is the corresponding estimated value,  $K_{undersampled}$  is a scalar that controls how far out on the tail of the residual distribution we wish to be (*i.e.*, it translates the maximum residual into one-sigma numbers and has, in practice, a nominal value is 5.33), and  $\sigma_{IPP_\kappa}^2$  is the inflated uncertainty of the delay estimate at the IPP. Under nominal conditions this inequality should always be satisfied. Under disturbed conditions, however, it may fail. When this occurs, we define  $\sigma_{decorr, IPP_\kappa}^{undersamp}$  by requiring

$$|I_{IPP_\kappa} - \tilde{I}_{IPP_\kappa}|^2 = K_{undersampled}^2 \left[ \sigma_{IPP_\kappa}^2 + \left( \sigma_{decorr, IPP_\kappa}^{undersamp} \right)^2 \right]$$

In constructing an ionospheric threat model, the objective is to determine the maximum values of  $\sigma_{decorr, IPP_\kappa}^{undersamp}$  ever observed (filtered by the disturbance detectors described below) as a function of the distribution of the IPPs in the vicinity of IPP.

In order to improve system availability under nominal ionospheric conditions, the GIVE algorithm allocates a portion of the integrity burden of protecting against undersampling ionospheric irregularities to two disturbance detectors: the irregularity detector at the IGP described previously and the system-wide *Extreme Storm Detector* (ESD) [7]. The ESD is driven by a metric based on the irregularity metrics from all the IGPs. When the

ESD is tripped, the GIVEs at all IGPs are increased to 45 meters for an extended period of time. The ESD protects against the extreme gradient threats that occur during and after extreme storm events, such as the Florida event observed during the Halloween storm of 2003. The threat model does not need to protect against undersampled threats that occur if either the irregularity detector at the IGP is tripped or the ESD is tripped, since the GIVE at the IGP is increased to its maximum 45 meter value under these conditions. Therefore, these threats are excluded from the undersampled threat model.

The raw data for the undersampled ionospheric threat model consists of  $\sigma_{decorr, raw}^{undersamp}$  tabulated as a function of the two metrics characterizing the IPP distribution in the neighborhood of the IGP (see Fig. 3), namely, the fit radius ( $R_{fit}$ ) and the relative centroid metric ( $RCM$ ). Tabulation of raw data is performed using the following equation:

$$\sigma_{decorr, raw}^{undersamp}(R_{fit}, RCM) = \max_{\text{over } \kappa, T} \sqrt{\frac{|I_{IPP_\kappa} - \tilde{I}_{IPP_\kappa}|^2}{K_{undersampled}^2} - \sigma_{IPP_\kappa}^2}$$

where the expression defining  $\sigma_{IPP_\kappa}^2$  is similar to that for  $\sigma_{IGP}^2$ , but evaluated at the IPP position, and the maximization is performed over measurements  $\kappa$  and over the time interval  $T$  following each fit.  $T$  accounts for GIVE computational latency, system broadcast latency, and message latency within the user receiver.

Figure 8 shows the tabulation of values of  $\sigma_{decorr, raw}^{undersamp}$  for the current WAAS ionospheric threat model. Fig. 9 shows the corresponding plot for the new threat model based upon kriging. The same data set is used to generate each figure, namely, the twenty-one days from the largest storms of the last solar cycle discussed in the introduction.

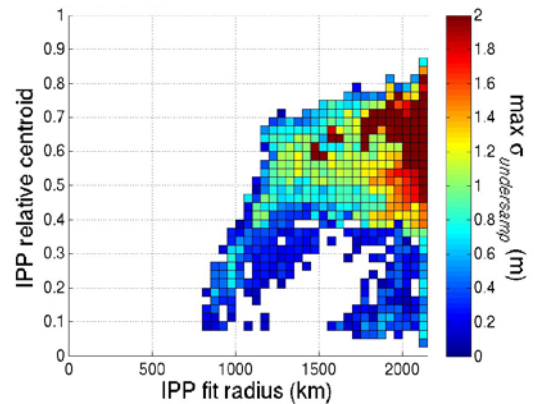


Figure 8: Raw data for the ionospheric threat model based upon planar fits.

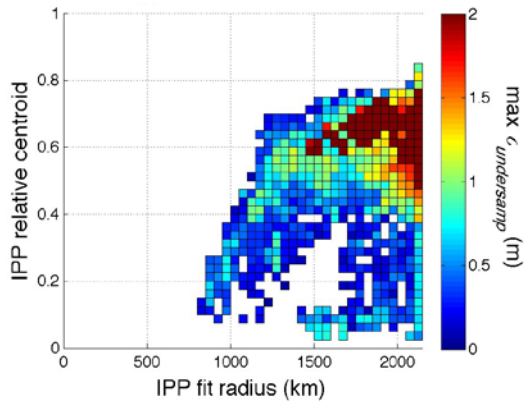


Figure 9: Raw data for the WAAS WFO Release 3 ionospheric threat model based upon kriging.

The actual threat model used by WAAS is defined as the two-dimensional overbound of the raw data. This ensures that  $\sigma_{undersamp}^{decorr}$  is monotonically increasing with respect to each IPP distribution metric. Figure 10 shows the current ionospheric threat model, and Fig. 11 displays the WFO Release 3 threat model. Notice that the two threat models closely resemble one another.

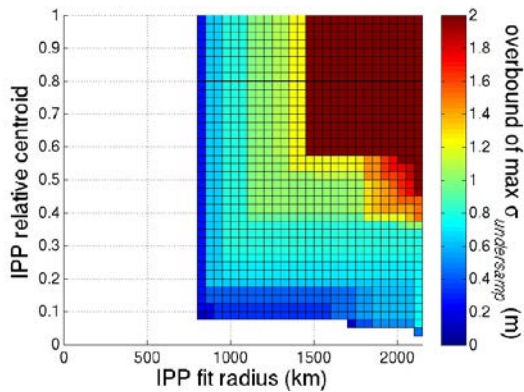


Figure 10: Current WAAS ionospheric threat model based upon planar fits.

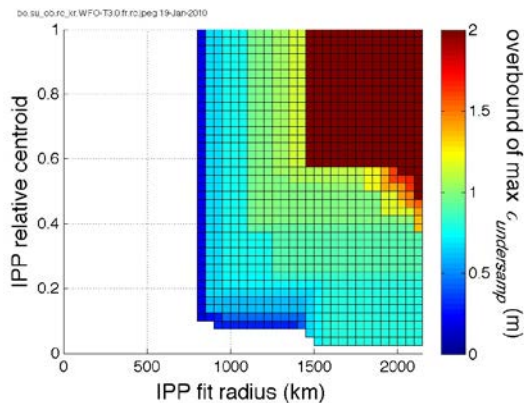


Figure 11: The WAAS WFO Release 3 ionospheric threat model based upon kriging.

## THE IMPACT OF KRIGING ON AVAILABILITY

Aviation service availability at a given user location can be quantified in terms of the user's computed Vertical Protection Limit (VPL) relative to a Vertical Alert Level (VAL), specified for a given level of aviation service. The VPL is defined as the MOPS receiver-computed integrity bound on the vertical region, centered on the user's location, in which the WAAS estimate of this location can be reliably assumed to lie within a required probability. WAAS is said to broadcast Hazardously Misleading Information (HMI) when the true error is larger than the VAL (for equipment aware of the navigation mode) or larger than the computed VPL (for equipment not aware of the navigation mode) without any notification of the error to the user within the time-to-alert of the applicable phase of flight. If the VPL exceeds the VAL, the given level of aviation service is not available to the user. Regional availability is quantified by the fraction of the day when the VAL specified for a given level of aviation service is greater than the user's computed VPL.

Since the user's computed VPL depends upon the GIVES at IGP's used to interpolate to the user's IPPs, two conditions must be satisfied at an IGP for the vertical delay at that IGP to substantially contribute to the computation of the users position estimate for a given level of aviation service:

1. the computed error bound at the IGP must not exceed a limit required by the desired level of aviation service;
2. the irregularity detector at the IGP or the ESD must not be in a tripped state.

If either of these conditions is not satisfied, the level of aviation service can be considered to be unavailable at that IGP.

To understand the impact of kriging on availability, one must consider both its effect on delay estimation accuracy and its affect on the ionospheric threat model. Kriging's ability to reduce estimation error promotes the availability of a given level of service for two reasons:

1. kriging reduces the magnitude of the inflated formal error, making it less likely that the VPL at the IGP will exceed the VAL;
2. kriging reduces the frequency that the irregularity detector trips.

From these considerations alone, one would expect kriging to improve WAAS availability.

The impact of kriging on the ionospheric threat model is more subtle. By reducing the magnitude of residual errors,

kriging is found to reduce the overall number of  $\sigma_{decorr, IPP_x}^{undersamp}$  values that are tabulated in the raw threat model data (*i.e.*, the number of values greater than zero). However, the threat model is determined by the maximum  $\sigma_{decorr, IPP_x}^{undersamp}$  value as a function of the two IPP distribution metric values ( $R_{fit}$ ,  $RCM$ ), and this maximum is not significantly affected by kriging. Figures 12 and 13 compare the distributions of  $\sigma_{decorr, IPP_x}^{undersamp}$  values that result from planar fit estimation and kriging estimation, both using storm data from October 30, 2003. The maximum value, mean value and standard deviation for the former are 5.48, 1.28, and 0.94, respectively, while the same values for the latter are 4.96, 0.91, and 1.24, respectively. Clearly the tails of these two distributions do not differ significantly.

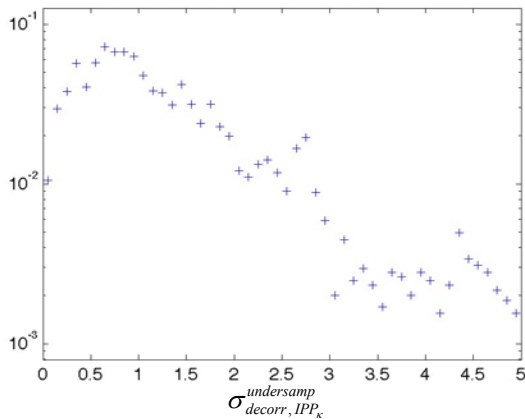


Figure 12. The distribution of  $\sigma_{decorr, IPP_x}^{undersamp}$  for data from October 30, 2003 using planar fit estimation.

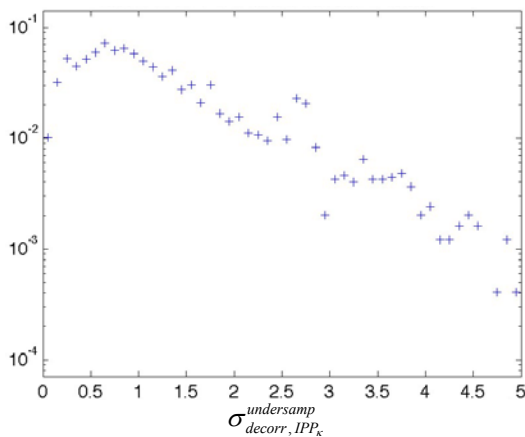


Figure 13. The distribution of  $\sigma_{decorr, IPP_x}^{undersamp}$  for data from October 30, 2003 using kriging estimation.

To this point, it appears that kriging affects availability solely due to its affect on delay estimation accuracy and not at all due to any affect on the threat model. This is somewhat of an oversimplification, however. Recall that the GIVE algorithm allocates a portion of the integrity

burden for detecting undersampled irregularities to the disturbance detectors. Therefore, each threat model is also dependent upon the choice of  $T_{irreg, trip}$ , the trip threshold for the irregularity detector. It has been found that kriging allows use of a higher threshold value. For the current threat model displayed in Fig. 10,  $T_{irreg, trip} = 2.5$ , while for the threat model based upon kriging shown in Fig. 11,  $T_{irreg, trip} = 3.0$ .

The advantage of using a higher threshold value is that the irregularity detector at each IGP will trip less often, aiding availability during disturbed ionospheric conditions. The potential disadvantage of raising the threshold is that more threats are tabulated in the threat model. At some point, these additional threats will cause the  $\sigma_{decorr}^{undersamp}$  values to become unacceptably large, *i.e.* their inclusion in the GIVE will increase the frequency with which the user VPL exceeds the VAL for nominal ionospheric conditions. Studies have shown that the implementation of kriging permits raising the threshold to  $T_{irreg, trip} = 3.0$  without adversely modifying the threat model significantly. In essence, the greater accuracy of the kriging model can be used to transfer some of the integrity burden for detecting undersampled irregularities back from the irregularity detector to the undersampled ionospheric threat model.

The Raytheon Service Volume Model (SVM) has been used to evaluate the fraction of the service volume for which a given aviation service is available, where availability is specified in terms of the fraction of the day when the Vertical Alert Limit (VAL) for the service bounds the user's VPLs. The results for Localizer Performance with Vertical guidance (LPV) service (VAL = 50 meters, decision altitude of 250 feet) and for LPV200 service (VAL = 35 meters, decision altitude of 200 feet) are presented in Table 1. Implementing kriging improves slightly the fraction of North America experiencing 100% availability for LPV service under nominal ionospheric conditions. The improvement is significantly greater for LPV200 service under nominal ionospheric conditions. The improvement is greater still for both levels of service under disturbed ionospheric conditions.

Conditions	Planar fit	Kriging
<i>LPV (VAL = 50 m)</i>		
Nominal ionosphere	88.8%	92.2%
Moderately disturbed ionosphere	79.1%	91.4%
<i>LPV200 (VAL = 35 m)</i>		
Nominal ionosphere	66.5%	75.5%
Moderately disturbed ionosphere	56.6%	71.9%

Table 1. The fraction of North America experiencing 100% WAAS availability on a day of nominal activity (July 8, 2009) and a day of ionospheric disturbance (July 22, 2009) for LPV and LPV200 services.

## CONCLUSIONS

The next release of WAAS will use kriging to estimate vertical delay values and their uncertainties. Kriging improves the accuracy of delay estimates while having little effect on the undersampled ionospheric threat model. WAAS availability will improve as a consequence of smaller estimation error and less frequent tripping of the irregularity detector.

## ACKNOWLEDGMENTS

The research of Lawrence Sparks was performed at the Jet Propulsion Laboratory/California Institute of Technology under contract to the National Aeronautics and Space Administration and the Federal Aviation Administration.

## REFERENCES

- [1] *Minimum Operational Performance Standards for Global Positioning System/Wide Area Augmentation System Airborne Equipment*, (WAAS MOPS), RTCA Document Number DO-229C, 28 November 2001.
- [2] Paredes, E., Pandya, N., Sparks, L., Komjathy, A., "Reconstructing the WAAS Undersampled Ionospheric Gradient Threat Model for the WAAS Expansion into Mexico", *Proceedings of ION GNSS 2008*, Savannah, GA, September 2008.
- [3] Wackernagel, Hans, *Multivariable geostatistics: an introduction with applications*, third edition, New York: Springer-Verlag, 2003.
- [4] Blanch, J., "Using Kriging to Bound Satellite Ranging Errors Due to the Ionosphere". Doctoral dissertation. Stanford University, December 2003.

- [5] T. Walter, A. Hansen, J. Blanch, P. Enge, A. Mannucci, X. Pi, L. Sparks, B. Iijima, B. El-Arini, R. Lejeune, M. Hagen, E. Altshuler, R. Fries, and A. Chu, "Robust Detection of Ionospheric Irregularities," *Proceedings of ION GPS 2000*, Salt Lake City, UT, September 2000.
- [6] T. Walter, S. Rajagopal, S. Datta-Barua, and J. Blanch, "Protecting Against Unsourced Ionospheric Threats," *Beacon Satellite Symposium 2004*, Trieste, Italy, October, 2004.
- [7] L. Sparks, A. Komjathy, A.J. Mannucci, E. Altshuler, T. Walter and J. Blanch, M. Bakry El-Arini and R. Lejeune, "Extreme Ionospheric Storms and Their Impact on WAAS," *Ionospheric Effects Symposium*, Alexandria VA, May, 2005.